Received: 5 January 2021 | Revised: 15 May 2021 | Accepted: 31 May 2021

IET Biometrics

DOI: 10.1049/bme2.12050

The Institution of Engineering and Technology WILEY

ORIGINAL RESEARCH PAPER

EEG personal recognition based on 'qualified majority' over signal patches

Andrea Panzino | **Giulia Orrù** | **Gian Luca Marcialis** | **Fabio Roli**

Department of Electrical and Electronic Engineering (DIEE), University of Cagliari, Cagliari, Italy

Correspondence

Giulia Orrù, Department of Electrical and Electronic Engineering (DIEE), University of Cagliari, 09123, Cagliari, Italy.
Email: giulia.orru@unica.it

Abstract

Electroencephalography (EEG)-based personal recognition in realistic contexts is still a matter of research, with the following issues to be clarified: (1) the duration of the signal length, called 'epoch', which must be very short for practical purposes and (2) the contribution of EEG sub-bands. These two aspects are connected because the shorter the epoch's duration, the lower the contribution of the low-frequency sub-bands while enhancing the high-frequency sub-bands. However, it is well known that the former characterises the inner brain activity in resting or unconscious states. These sub-bands could be of no use in the wild, where the subject is conscious and not in the condition to put himself in a resting-state-like condition. Furthermore, the latter may concur much better in the process, characterising normal subject activity when awake. This study aims at clarifying the problems mentioned above by proposing a novel personal recognition architecture based on extremely short signal fragments called 'patches', subdividing each epoch. Patches are individually classified. A 'qualified majority' of classified patches allows taking the final decision. It is shown by experiments that this approach (1) can be adopted for practical purposes and (2) clarifies the sub-bands' role in contexts still implemented in vitro but very similar to that conceivable in the wild.

1 | INTRODUCTION

In recent years, with the digitisation of many sectors (private, public, educational and government), biometric authentication has become essential, to guarantee an adequate level of reliability and security.

Electroencephalography (EEG) signals as biometrics are more secure and privacy compliant than well-known ones such as the fingerprint and the face. They cannot be attacked with *spoofs*, due to the inability to acquire the signal remotely [1, 2]. Moreover, the risk of circumvention is minimum: if a subject is forced to provide his own EEG signal, this would be unusable for the purpose of authentication due to the induced stress [3].

Although authentication via EEG has achieved encouraging results, especially after the spread of deep learning methods, its real application needs further refinements [4–6]. Many state-of-the-art (SOTA) methods, although accurate, suffer from the continuous changes of human states, due to physical movements and psychological conditions. Moreover, the acquisition time required for obtaining a useful sample, called epoch, has an impact on the user's acceptability. To the best of our knowledge, the smallest duration of an epoch is 1 s [7], whilst other competitive systems require 12 s [8, 9]. Among problems, the lack of robustness under realistic conditions of use, the so-called cross-tasks problem, is still unsolved, despite the noticeable results obtained by functional connectivity measurements [10] and graph-based deep networks [2].

On the basis of our previous works, which showed that the fusion of multiple matchers can help even in EEG-based personal recognition based on functional connectivity measurements [11, 12] and the sharp potentials of deep learning shown in [2, 7], we propose an EEG-based personal identification system based on the fusion of the classification over multiple *patches*. By this term, we mean very short portions of the electroencephalographic trace. These are represented as pseudo-images and used as the input of a convolutional neural network (CNN). The immediate advantage is that we need fewer samples to train a CNN, due to each patch's size (about

60 ms per patch or even less according to our experiments), as well as a smaller network. According to the user population size, the output is interpreted as the set of probabilities that the patch belongs to, for each subject. The final classification is obtained by a decision-level fusion algorithm applied to the patches of the same EEG sample (epoch). Our fusion algorithm combines the consensus voting rule with a threshold-based selection of decision. In other words, we obtain a 'qualified majority' when the number of collected patches exceeds a pre-set value.

We show that our approach achieves performance comparable or better than that of other state-of-the-art ones. The reduced time size of the epochs assures good user acceptability. The system can also deal with enrolled and unenrolled people (closed and open set). Evaluation of the performance of unenrolled people allows us to avoid the overestimation of the identification accuracy [2]. Moreover, as the EEG signal is particularly influenced by the onset of emotions [13–15] and by motor or visual activities, one of the aims of this study is to present a robust recognition approach to such intra-class variations. In fact, the maintenance and exploitation of the high frequencies obtained through the shortness of the patches made the system robust under the cross-tasks test, that is, when training and test conditions differed from each other, thus simulating realistic contexts of use. In a few words, we propose a system much simpler than that of Ref. [2] and better in accuracy than others exhibiting similar network architectures [7]. It can maintain very high identification accuracy over short epochs, according to the state of the art. Finally, the recognition time, which depends on the relationship between the classification of a certain patch and the acquisition of the next one, can be further reduced, thanks to the threshold-based voting rule.

The rest of this study is organised in the following sections: Section 2 describes the purpose of the experimentation and the proposed method. The experimental methodology, results and concluding remarks are presented in Sections 3 and 4, respectively.

2 | EEG PERSON IDENTIFICATION BY DECISION-LEVEL FUSION OF MULTIPLE PATCHES

We propose an EEG-based person identification system based on the decision-level fusion of the classification over multiple *patches*. The proposed system, schematised in Figure 1, is composed of two modules, a first classification carried out with a CNN, which divides the signal into fragments, and a second classification, called single threshold classification, based on decision-level fusion, which gives the system the ability to reject a user and allows us to adopt the identification system in real applications. The choice of a CNN architecture allows us to obtain a performing system with a faster and more efficient computation compared to more complex solutions, as we have highlighted in Section 2.2. In particular, the CNN classification module takes a 1-s EEG signal in input and returns N scores on the basis of the subdivision into N fragments called 'patches', described in Section 2.1. The output is their posterior probability computed by a CNN described in Section 2.2. The threshold classification module takes the N probabilities as input and returns the user's identity or rejects the user as unknown. This final decision depends on whether the maximum posterior probabilities of each patch converge over a certain subject or not. This approach, which we call decision by 'qualified majority', is described in Section 2.3.

2.1 | Patch definition

The EEG signal is the recording of the brain's electrical activity due to the ionic current within the neurons [16]. It is possible to categorise these signals according to their frequency ranges into five frequency bands that correspond to different mental states: Delta (<4 Hz), Theta (4–8 Hz), Alpha (8–13 Hz), Beta (13–30 Hz) and Gamma (30–100 Hz) [17].

In pattern recognition and artificial intelligence applications of the EEG signal, it is common to consider a pre-set time-length sample, called 'epoch' [18]. For the length of one

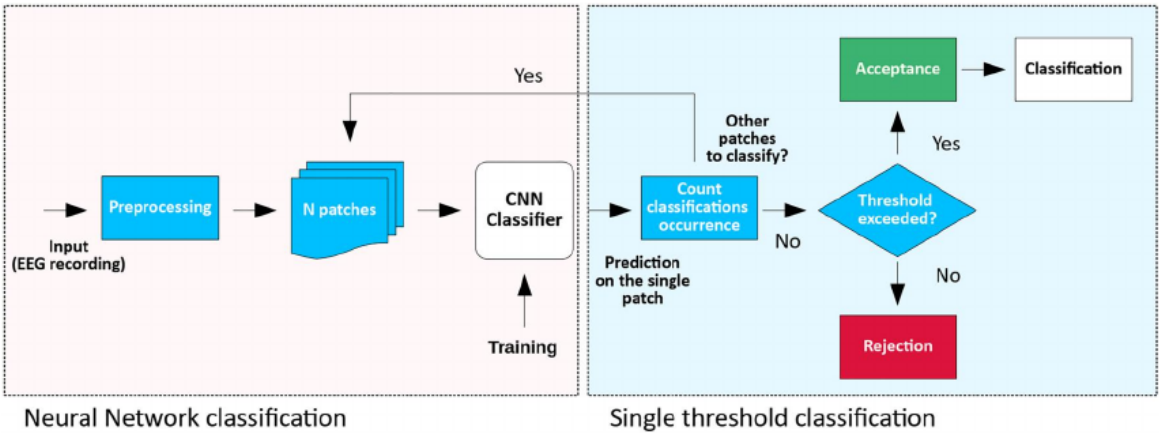

FIGURE 1 Graphical representation of the proposed identification system. The system classifies patch fragments and bases the final decision on a qualified majority

epoch, the particular phenomenon of interest is studied. This has also been done for personal identification [19, 20].

An epoch should be long enough to capture the signal frequencies of interest: generally, the low frequencies, which traditionally are intended to embed the neural cortical activity. However, a person recognition system must work in realistic environments where people cannot be hypothesised under resting state or when carrying on a few of very specific tasks. Let us think about using the EEG to drive a certain interface—open a door or recognise that the person in front of him is a friend.

Therefore, the need for considering the full amplitude of an EEG signal, between 1 and 80 Hz, is necessary. In particular, we want to demonstrate that person identification can be done by subdividing an epoch into extremely short temporal fragments, thus enabling the frequencies at the border of the EEG spectrum to face more realistic contexts of use.

We consider epochs of 1 s; after filtering the frequencies below 1 Hz, we divided it into N equal fragments, which we called 'patches', as is usually done in other works [21–23]. To the best of our knowledge, this is the first time that the term 'patch' is being used in the context of the EEG signal, even if the division of the EEG signal into various smaller portions has already been investigated by Lan Ma et al. [7] with the purpose of finding whether the minimum temporal length of the signal is still able to preserve the identification information or not. However, Lan Ma's method uses the signal fragment as the EEG epoch and has no classification fusion system.

Each patch is represented by pseudo-images obtained by mapping the EEG channels into time series of 2-D mesh as in [2, 7]. Therefore, the CNN input is a patch of size $c \times i$, where c is the number of channels and i is the number of sampling instants, obtained from the time length of the patch l and multiplied by the sampling frequency f. Figure 2a shows an example of a patch related to a 64-channel signal, sampled at 160 Hz and 0.0625 s long. In this specific example, the size of the input image to the network is 64×10, since $i = l \cdot f = 160 \cdot 0.0625 = 10$.

We normalised each patch value by *Min–Max* normalisation in order to avoid any spurious correlation between the channel components.

Using 'patches' instead of epochs and their full extension has the following practical advantages: (1) we still exploit the temporal information without the need for further preprocessing or feature extraction steps and (2) we keep low the complexity of the selected classifier. In our case, a CNN like that described in Section 2.2. Its number of parameters being low, it can be easily led to overfit the training patches in order to have generally high estimated values of posterior probability.

The EEG signal is captured at a very high sampling frequency compared to the normal extension of the cerebral signal. The rationale behind signal patching starts with

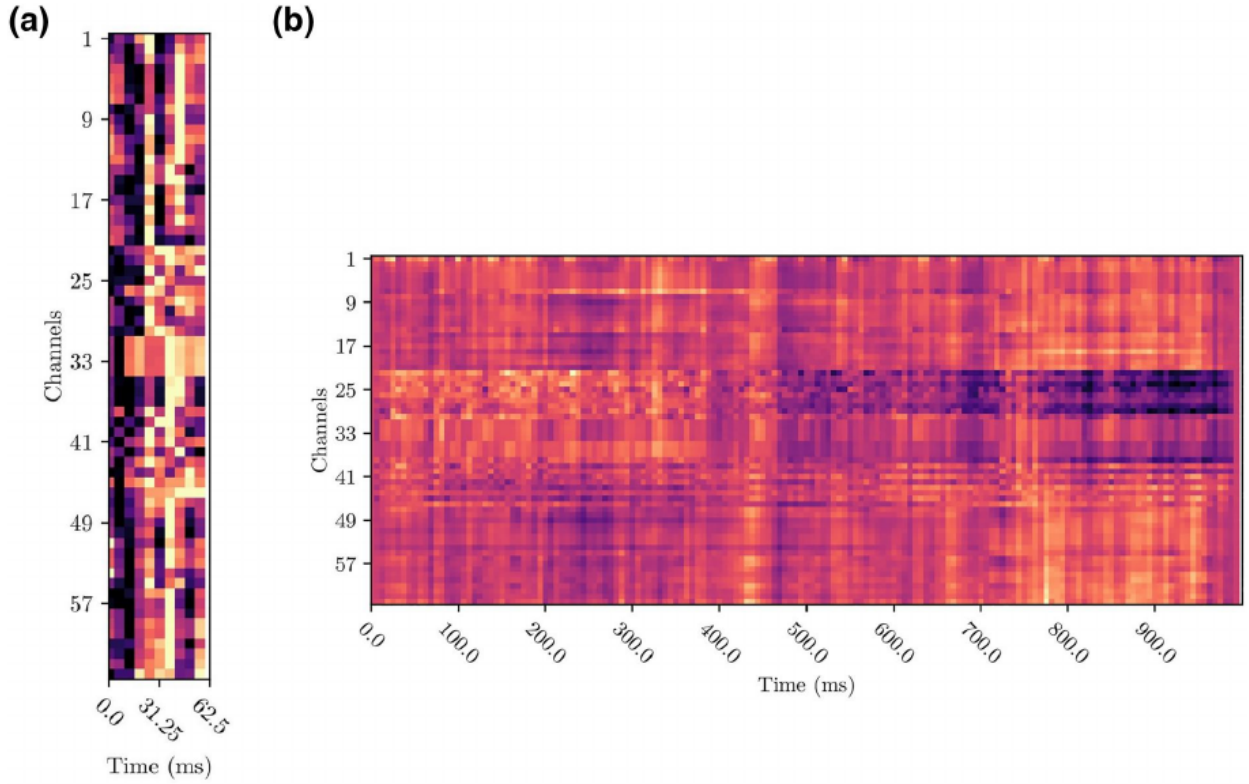

FIGURE 2 Image (a) is the patch input to the system. In (b), the set of N patches that constitute an epoch (1 s) on which the decision is made through 'qualified majority'. In this specific example, the size of the input image to the network is 64×10, since $i = l \cdot f = 160 \cdot 0.0625 = 10$. The patch number N equals the length of the epoch divided by the length of the single patch. In the example shown, an epoch of 1 s is divided into 16 patches of 0.0625 s

characterising the signal into sub-bands. Five sub-bands describe some physiological and behavioural states [24]:

- Gamma (30–90 Hz): learning, heightened perception and REM sleep until high arousal and stress in case of large amplitude.
- Beta (13–30 Hz): normal alertness while awake, until stress in case of large amplitude.
- Theta (4–8 Hz) and Alpha (8–13 Hz): relaxed or day-dreaming, drowsy state, until the inability to focus in case of large amplitude.
- Delta (below 4 Hz): deep sleep, healing repairs body until the inability to think or learn in case of large amplitude.

Based on very short patches, the proposed method aims to make the system robust to intraclass variations and at the same time discriminate users. The system is not expected to respond in sleep states in the field of identification. For this reason, we are not interested in low frequencies but in highs, such as Gamma and Beta. The signal fragments of the order of milliseconds cut a significant component of the low frequencies. The very low frequency Delta and Alpha bands are the ones that most determine the states of deep sleep but do not characterise activity in the waking state [25]. Cutting the contributions of low frequencies allows us to obtain a realistic descriptor and, at the same time, multiple fragments that lead to a more precise identification. The use of very short signals leads to a greater characterisation of the Gamma and Beta bands and allows us to keep the input of the neural network small.

Moreover, in the field of personal recognition, often the Gamma band and more commonly the high frequencies of the Gamma band, above 40–50 Hz, are filtered [9, 19], as they are overlapped on the electrical activity that muscle activity produces (20–300 Hz) [26]. However, these high frequencies contain information and characterizes, in addition to the activity of the motor cortex, the visual cortex and the onset of emotions [26–28]. Starting from the assumption that the neural network can exploit this information that characterises the realistic use of the recogniser to learn and filter this information when not useful, we have considered the signal filtered at 80 Hz and not at 50 Hz, like many other state-of-the-art works. To corroborate these assumptions, we analysed the contribution of each band and the contribution of high frequencies in Section 3.3. The additional information about high frequencies allows the system to be more robust against outliers caused by realistic variations in the signal, such as emotions and motor or visual activities. The datasets used to evaluate the system's performance, described in Sections 3.1 and 3.2, allow us to ascertain the cross-task robustness of the system, simulating these variations.

2.2 | CNN architecture

The majority of the proposed EEG authentication systems are based on several signal processing techniques to perform feature extraction [9, 29–35]. Some of them are explicitly conceived to deal with EEG patterns [9, 10, 35]. However, most feature-based methods require epochs of 10 s or more [9, 10, 35] and are affected by changes in human states [10].

Deep-learning-based methods are increasingly used in the field of EEG signal processing and classification due to the compact and powerful representations they can provide [5]. CNN are adopted in [7, 36–38] and fed with static data, such as images or signal segments and allowed to achieve very accurate results with the closed set identification, that is, tested only on a set of enrolled subjects.

Recent studies [2, 19, 20, 39] have shown how hybrid neural architectures, such as a cascade of a CNN and an recursive neural network (RNN), exploit temporal information and present remarkable performances. However, these architectures have high computational complexities due to the presence of the 'Long Short-Term Memory' (LSTM) and 'Gated Recurrent Unit' (GRU) layers [2]. On the contrary, CNNs are the fastest ones even in the training phase [39] and their potential, in our opinion, has not yet been fully investigated. Therefore, we chose a CNN architecture for implementing the classification module. This choice allowed us to obtain a small, performing architecture, which exploits the temporal information of the input patches.

Our network (Figure 3) is made up of five layers: two convolutional layers alternated with the same number of max-pooling layers and a final dense layer. Eighteen square 5 × 5 size filters were used in the convolutional layers, while the

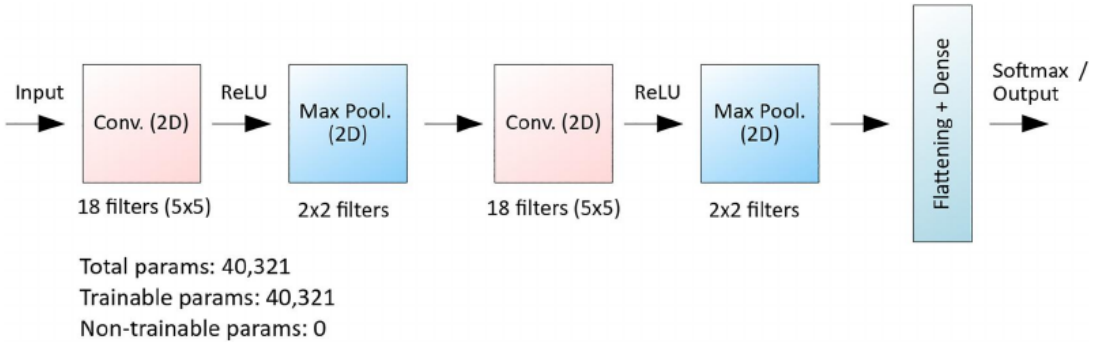

FIGURE 3 Schematic representation of the network architecture used

pooling was performed with 2 × 2 reduced size filters. As activation function, the *Rectified Linear Unit* (ReLU) was used as the output to the two convolutional layers, while *Softmax* was used in the case of the final dense layer. Although the OpenMax layer [40, 41] is preferred to the SoftMax one in open-set scenarios, we chose SoftMax for taking advantage of the posterior probability estimation, as explained in Section 2.3. The OpenMax, in fact, allows the rejection of images not related to those known by the system. So we move this decision to the threshold classification module.

The optimiser used for the network is *Adam* with a *Mean-Squared-Error* loss function. Although similar to that reported in [7], our network differs in terms of the number of filters in the convolutional layers (18 filters instead of 6), the type of padding (zero padding instead of valid padding) and that of pooling (max pooling layers instead of average pooling layers). Anyway, the CNN does not represent the core of our contribution.

2.3 | Decision by 'qualified majority'

CNN architectures with a final Softmax layer, as the one proposed, force linking the input sample to a registered user, even if it belongs to an unenrolled user. This allows the system to have a high accuracy of identification but it cannot reject impostors. For this reason, this kind of approaches usually require additional schemes to exclude the unregistered users, for example, a two-layer system as in [2].

The proposed method aims to simplify the dynamics behind the additional schemes mentioned above. In fact, Wang's method is composed of two neural networks in series, while we have replaced one of these networks with a decision-level fusion module [42]. This module is aimed at generating what we called 'qualified majority'.

Our goal is to lower the system's computational complexity and maintain high protection from intruders.

During the system's operations, the model operates N predictions, one per patch. These predictions are interpreted as the set of posterior probabilities of each enrolled subject for which the patch is given. For the final classification, the subject with the highest occurrence is assigned. This is done under the condition that this occurrence has exceeded an *acceptance threshold*. In other words, we want to collect enough evidence about the targeted subject before the final decision, and this number must be more than the acceptance threshold in the worst case. If this does not happen, the epoch is classified as belonging to an unregistered subject and rejected (Figure 1).

In other words, we rely on a 'qualified majority' around the targeted subject before making a decision. The Softmax layer outputs posterior probabilities close to the extremes of the activation function of the prevalent output neuron. Applying a threshold to the maximum number of 'votes' has two relevant implications and adds a novel contribution to the state of the art. First, it manages both unenrolled users and intra-class variations of enrolled users. Second, it allows the whole EEG signal processing pipelining, from its acquisition to its classification.

The subdivision of the epoch into patches allows us to have more information to make the decision. The CNN extracts features from the raw input and then computes the decision surface according to the given classes (users). Therefore, the decision surface describes exactly what the neural network has stored on exploiting the training samples, that is, the patches from each user. This implies that the neuron activated by the SoftMax layer exhibits a very high value. In other words, the associated posterior probability is near to 1, even in case of bad estimation. It is easy to see that the sum of these values approximates the majority voting rule; thus, the output of the rule is equivalent to computing the average or the sum [43]. Moreover, the decision scheme is strictly linked with Wald's sequential hypothesis verification test, where the number of pieces of evidence corresponds to the size of the 'qualified majority', that is, the number of 'votes'. Whichever the way of looking at our decision rule based on the 'qualified majority' over multiple patches is, namely, as the sum of posterior probabilities or as the collection of incremental pieces of evidence, a large literature has shown that these are the best and most robust approaches for dealing with first- and second-type errors [43].

3 | EXPERIMENTAL RESULTS

3.1 | Physionet EEG database

The first dataset used in this work is the *Physionet Motor/Imagery Dataset* [44, 45]. This dataset is made up of EEG recordings from 109 subjects. Signals are acquired using 64 electrodes under the 10-10 configuration.

A total of 14 recordings, each sampled at 160 Hz, was made for each subject. These include six different tasks, which are listed below:

1. Resting State with Eyes Open (REO)
2. Resting State with Eyes Closed (REC)
3. Open and close left or right fist (PHY_FI)
4. Imagine opening or closing left or right fist (IMA_FI)
5. Open and close both fists or both feet (PHY_FE)
6. Imagine opening or closing both fist or both feet (IMA_FE)

3.2 | DEAP database

To test our method in a different application context, we used the EEG signals of the *DEAP Dataset*, a multimodal dataset for emotion recognition or affective tasks [46]. Thirty-two subjects took part in the experiment. Their EEG signals were recorded while watching 40 selected music videos. They rated each video in terms of valence and arousal [47]. The research group that collected this dataset made available the pre-processed and segmented version of the EEG data, which

we used in this study. Each signal was downsampled to 128 Hz, EOG artefacts were removed and a bandpass frequency filter from 4.0 to 45.0 Hz was applied.[1] We resampled the signal to 160 Hz. We used the DEAP database to perform person identification because the recorded signals can be considered more realistic than the classical in vitro use case, namely, the resting state. This data\set was used for the same goal in [19]. In other words, we considered the emotional state as a task. The measures of valence and arousal scores reported are in the discrete range {1, 9}. As in Ref. [19], we labelled the video as 'Low' if the score was less than 5 and 'High' if the valence-arousal scores were greater than or equal to 5, obtaining four tasks: Low Valence and Low Arousal (LL), Low Valence and High Arousal (LH), High Valence and Low Arousal (HL) and High Valence and High Arousal (HH).

We have selected four or five videos per status for each user, depending on their availability based on our subdivision. Participants who had fewer than four EEG recordings classified for a given task were discarded in the experiments involving that task.

For the cross-task experiments, we have selected the users available for both the train task and the test task. The number of users and the total number of videos for each experiment are shown in the Tables 1 and in 2, where the train task is indicated in the rows and the test task in the columns. The diagonal shows the values for the experiments in which the system is trained and tested on the same task (within task).

TABLE 1 Number of users for each experiment

Task	HH	HL	LH	LL
HH	31	27	27	26
HL	27	28	24	24
LH	27	24	28	23
LL	26	24	23	27

Notes: The rows indicate the train tasks and the columns the test tasks. In cross-task experiments, only users who have at least four videos in both the train and test tasks are used.

TABLE 2 Number of videos for each experiment

Task	HH	HL	LH	LL
HH	155	135	135	130
HL	134	139	119	119
LH	132	117	137	112
LL	130	120	115	135

Note: The rows indicate the train tasks and the columns the test tasks.

3.3 | Parameters setting: optimal time length per patch and band filtering

One of the contributions of this study is to evaluate an EEG-based person identification system that uses extremely short signal fragments in order to make the system more easily applicable in a real-world scenario. For this reason, we first assessed how much the temporal length of the patches and the EEG signal band, or rhythm, could impact the overall identification accuracy. In this regard, nine different lengths have been tested for each EEG band (Delta: 0.5–4 Hz, Theta: 4–8 Hz, Alpha: 8–13 Hz, Beta: 13–30 Hz, Low Gamma: 30–40 Hz or Broadband signal 1–80 Hz).

For this evaluation, a five-fold cross-validation was carried out on 55 users of the Physionet dataset considering only the first 50 s of the REO recordings. We calculated the correct recognition rate, namely, the accuracy, on the individual patches as the ratio between the number of correctly classified patches and the total number of patches submitted.

Figure 4a shows that the system is able to perform accurate personal recognition through short signal fragments, which makes it extremely fast in use. In particular, the mean accuracy is higher for patches of 10 sampling instants (62.5 ms), which was used for the rest of the experiments.

As it is possible to notice, the best results were obtained through the use of the *broadband* signal, followed by the *beta* and *low gamma* bands, respectively.

This result is in complete agreement with [7, 35] that show how the broadband can lead to better results in terms of identification accuracy.

To assess whether high frequencies were actually useful in personal identification, we compared the accuracy using 1–80 Hz and 1–50 Hz filtering. The results, shown in Figure 4b, confirm that high frequencies contribute positively to personal recognition.

Figure 4a also highlights that low frequencies, that is, delta, theta and alpha, cannot be exploited on very short signals. We wanted to analyse if the filtering of these frequencies could lead to an improvement in recognition accuracy. For this reason, the system's accuracy with different filterings is shown in Figure 4c. For the chosen patch length (62.5 ms), filtering does not affect performance. Only frequencies above 40 Hz have a significant contribution. On the other hand, the lower frequencies appear to be completely cut and 'disturb' the signal from a patch length of 312.5 ms. The accuracy drastically drops, probably due to the noise overriding the informative content. These results confirmed our initial hypothesis that the high gamma band (above 50 Hz) is decisive for identification. They are usually cut off because they suffer from the activity of the motor and visual cortex. In our opinion, neural networks are able to exploit this information, learning to filter it when not needed and making the system more robust to intraclass variations. On the basis of the above results, we kept the broadband signal (1–80 Hz), which avoids a further and unnecessary filtering step without affecting the final performance.

[1]Further information on data pre-processing can be found in http://www.eecs.qmul.ac.uk/mmv/datasets/deap/readme.html.

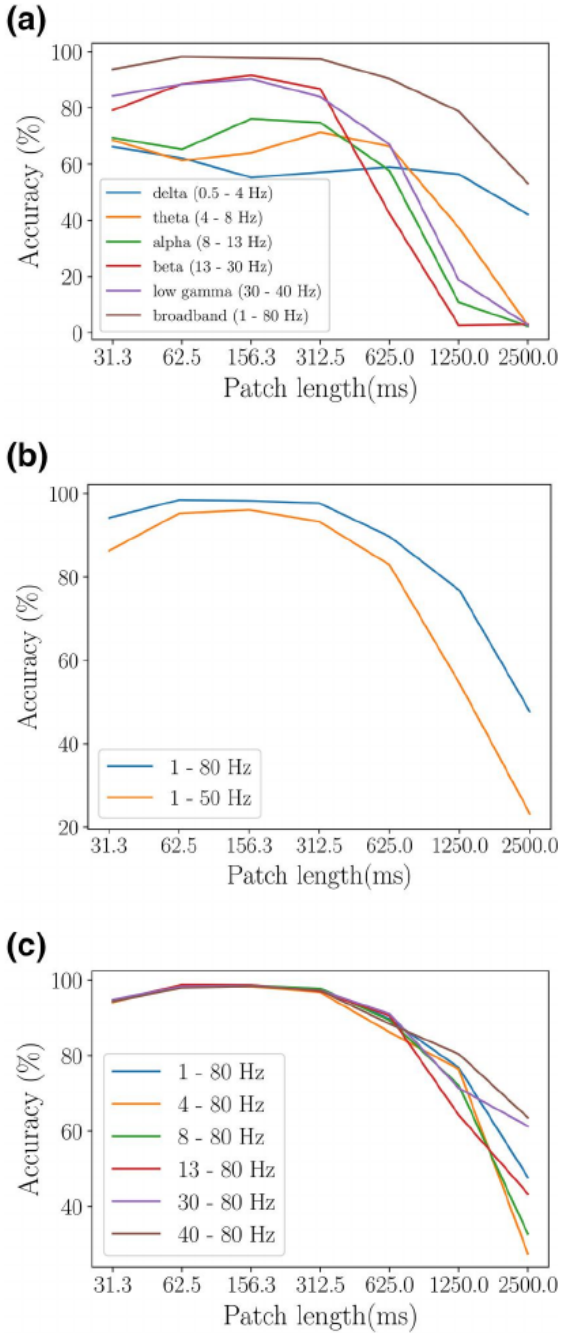

FIGURE 4 Assessment of the impact of patch length and filtering band on system performance using the Physionet dataset

3.4 | Closed-set, open-set and cross-tasks experiments

Two experiments were designed to test the proposed patch-based EEG personal recognition system in different human states. In the *within-task* case, train and test are on the same task type recordings. In the *cross-task* case, train is on a task type recording and test on different ones.

Two protocols were used for the performance evaluation, with slight variations according to the dataset. Due to their different composition, the protocols vary according to the dataset. For all protocols and datasets, a 1-s epoch that is divided into 16 patches and is 62.5 ms long was considered.

3.4.1 | Closed-set protocol

The performance was evaluated by training the network on all the subjects. Only enrolled users were in the test set. The adopted datasets were treated as follows:

- Physionet: We did 10 runs, using five-sixths of the signal selected randomly to train the network (40 s for the training set and 10 s for the validation set for each recording) and the remaining one-sixth, equal to 10 s for each recording, to test it.
- DEAP: Two or three videos were used to train, one for the validation set and one for the test set. Ten runs were carried out. Consequently, users with less than four EEG recordings classified in a certain task were discarded.

3.4.2 | Open-set protocol

Both enrolled and unenrolled users were in the test set. Accordingly, the subjects in each dataset were randomly subdivided into two groups, alternatively considered as the set of enrolled users and the set of unenrolled users. The neural network was trained only on the set of enrolled users. Ten runs were carried out, randomly sampling N_{enr} subjects for the enrolled users' set and the remaining subjects for the unenrolled users' set. The adopted datasets were treated as follows:

- Physionet: We chose $N_{enr} = 55$ and $N_{enr} = 80$, for the sake of comparison with Ref. [2]. In both cases, we trained the network on 50 s of recordings (40 s for the training set and 10 s for the validation set for each recording) and tested on the following 10 s per task. Therefore, we only consider 10 s of recording for the unenrolled users' set, as these users were not used to train the network. The use of two values of N_{enr} allowed us to evaluate the system's scalability. It should be noted that in a real application the addition of enrolled users in the system entails retraining of the network, constituting a limit of the proposed system.
- DEAP: We set N_{enr} such that its percentage over the users per task was 75%. Two or three videos were used to train, one for the validation set and one for the test set. Therefore, we only consider one video for the unenrolled users' set as these users were not used to train the network. The videos were randomly selected from those available and the experiment was repeated 10 times.

3.4.3 | Performance metrics

As explained in the previous section, the epoch is associated with an enrolled user, or not, depending on the system's output. The system identifies each individual in the test with a 1: N comparison. For this reason, the typical identification

metrics defined by the ISO/IEC 19795-1: 2006 standard [48] were used, namely, false-negative identification-error rate (FNIR), false-positive identification-error rate (FPIR) and correct (true-positive) identification rate (CIR). In particular, if the epoch is from an enrolled user, three cases may occur: (1) the association is correct, (2) the association is incorrect or (3) no association is given. According to [49], we referred to the above cases as the number of correct identifications (CI), the incorrect identifications (FNEI) and the false-negative identifications (FNIU), respectively. Therefore,

$$CIR = 100 \cdot \frac{CI}{CI + FNEI} \quad (1)$$

$$FNIR = 100 \cdot \frac{FNIU}{CI + FNEI + FNIU} \quad (2)$$

If the sample is from an unenrolled user (impostor), two cases may occur: (1) the association is incorrect or (2) no association is given. According to [49], we referred to case (1) as the number of false-positive identifications (FPI) and to case (2) as the number of true-negative identification (TNI):

$$FPIR = 100 \cdot \frac{FPI}{FPI + TNI} \quad (3)$$

$$Accuracy = 100 \cdot \frac{CI + TNI}{CI + FNEI + FNIU + FPI + TNI} \quad (4)$$

These parameters can be adapted to the closed-set case, by considering that no unenrolled users are considered, leading to $FPI = TNI = FNIU = 0$. Therefore, $CIR = Accuracy$ and $FPIR = FNIR = 0$. When reporting the closed-set results, we therefore refer only to *Accuracy* as the performance index, defined as the percentage of samples correctly recognised out of the total.

3.5 | Results

3.5.1 | Within-task

For the within-task experiment, we evaluated both protocols, closed set and open set.

The closed-set results for both Physionet and DEAP datasets are reported in Table 3, in comparison with the other methods at SOTA.

On the Physionet dataset, the proposed system is high performing, considering the very short length of the epoch. The other methods that exceed 99.90% accuracy use epochs longer than 10 s [20, 35].

In particular, the classification of a single patch was, in fact, very precise, reaching 98.25% of accuracy. This means that when the epoch time was reduced to that of one patch, the baseline was already very good and the accuracy was 99.90% if we took also into account up to the fifth activated neuron of the SoftMax layer.

The initial purpose of the DEAP dataset being different from that of individual recognition, for this set of data we directly compared our method with [19], which had previously performed this analysis. We replicated the experimental protocol, described in Sections 3.2 and 3.4. The within-task results in the closed set for the DEAP dataset are reported in detail in Table 4. Although 'simple', as it is composed of a CNN without the LSTM and GRU layers that involve a high computational complexity, the proposed method maintains the best performance on all four tasks. Also, for the DEAP dataset, the single patches' classification is very precise, exceeding 98.50% for all tasks. This shows that the system can

TABLE 3 Comparison with SOTA approaches in closed set protocol. The training task is indicated in the 'Task type' column

Method	Year	Classification	Dataset	Subjects	Channels	Task type	Accuracy	Epoch
[35]	2014	Distance-based	Physionet	108	56	REC	100.00%	10 s
[9]	2015	Distance-based	Physionet	109	64	REO	96.90%	12 s
[7]	2015	CNN	Physionet	10	64	REO	88.00%	1 s
[50]	2016	LDA	Physionet	108	9	REO	96.15%	30 s
[36]	2017	CNN	BCIT	100	64	Drive	97.00%	1 s
[37]	2017	CNN	-	40	17	VEP	99.80%	0.6 s
[38]	2018	CNN	SSVEP	10	-	VEP	95.90%	1 s
[19]	2018	CNN/GRU	DEAP	32	32	LL	99.90%	10 s
[39]	2019	CNN/LSTM	Physionet	109	16	Multi-tasks	99.58%	1 s
[20]	2019	CNN/LSTM	Physionet	109	64	REO	99.95%	12 s
[2]	2019	GCNN	Physionet	109	64	REO	99.75%	3 s
[35]	2020	Graph-based	Physionet	109	64	REO	98.83%	1 s
Proposed	2021	CNN	Physionet	109	64	REO	99.91%	1 s
Proposed	2021	CNN	DEAP	32	32	LL	99.99%	1 s

also be used with epochs of less than one second while remaining efficient.

Furthermore, our approach shows its potential in open-set experiments. In fact, the 'qualified majority' allows us to reject all those epochs that cannot be unequivocally assigned to a registered user. The threshold, which defines the 'qualified majority', must be chosen on the basis of the application requirements. A stringent threshold allows fewer impostors to pass, decreasing the FPIR error and increasing the FNIR error. If the application needs high protection from impostors, it is better to use a stringent threshold to obtain the opposite effect. In general, a trade-off between FPIR and FNIR must be found.

Table 5 compares our results with the unique state-of-the-art work that tested the system under open-set conditions with a few details about the FPIR value [2]. In order to have a similar experimental protocol, we have combined the PHY_FI and PHY_FE tasks into a single PHY task and the IMA_FI and IMA_FE tasks into a single IMA task. It is not listed as Wang et al. [2] calculates FPIR (FAR in the study) or the corresponding system accuracy, we report in Table 5 the FPIR and the accuracy of the proposed method, with two different thresholds: the optimal one is calculated for each task in order to maximise the overall accuracy and a possible sub-optimal one over all tasks corresponding to 87.50% of the patches classifications agreement, that is, when 14 out of 16 patches were associated with the same decision. The table also shows how the system's performance changes based on the number of registered and unregistered users. We also notice that from 55 to 80 enrolled users, i.e. by a user number increase of 45%, the accuracy is almost unaltered. Therefore, the system is not affected by scalability problems in terms of accuracy. Of course, we have to retrain the system each time a novel user is added, and this may be considered a drawback that needs to be taken into account.

Regardless of how it is set, the presence of a threshold makes the classifications of the latest patches unnecessary in case the acceptance threshold is already exceeded and allows us to reduce the average recognition time per epoch. This aspect has been extended in Section 3.5.4. In the rest of the experiments, we used the optimal threshold within task, that is, we calculated the threshold based on the training task.

To our knowledge, no state-of-the-art work has evaluated recognition performance in open-set situations for the DEAP dataset. The diagonals of matrices in Figure 9 show the DEAP within-task results. In the open set, we have a decrease in performance of about three-fourths percentage points compared to the closed set, mainly due to impostors classified as genuine. The FNIR, on the other hand, remains below 1.3% for all tasks, except for the HH task (3.12%). On all the tasks, we obtain an accuracy of more than 95% and no enrolled user is confused with other users, having a CIR always equal to 100%.

TABLE 4 Comparison of the within-task results with SOTA approaches for the DEAP dataset in closed-set protocol

	Accuracy (%)			
Method	**LL**	**LH**	**HH**	**HL**
Proposed	99.97	100.00	99.99	99.99
CNN-GRU	99.90	99.71	99.86	99.87
CNN-LSTM	99.79	100.00	99.86	99.74

Abbreviations: CNN, convolutional neural network; GRU, Gated Recurrent Unit; LSTM, Long Short-Term Memory.

3.5.2 | Cross-task

Cross-task experiments were aimed at investigating if the decision-level fusion adopted is robust enough to handle 'less representative' patches due to changes in the human states. Figures 5 and 6 report the closed-set accuracy of the proposed approach on Physionet and DEAP dataset, respectively. Rows indicate the training condition and columns the testing condition. The accuracies on the diagonal correspond to the *within-task* experiments, analysed in Section 3.5.1. The values outside the diagonal refer to the *cross-task* evaluation, namely, training on a task (row number) and testing on another one (column number).

As expected, the cross-tasks values were averagely lower than within tasks' ones. This is particularly evident for the Physionet dataset, while in the case of the closed-set DEAP dataset, the error rate is almost zero for both within task and cross-task. On Physionet, for the closed set reported in Figure 5, we got the worst accuracy (82.63%) in the IMA-_FE-REC case and the best one (98.13%) in the IMA_FE-IMA_FI

TABLE 5 Comparison with SOTA approaches in open-set protocol for the Physionet dataset

			FPIR				Accuracy			
Method	**Enrolled users**	**Unenrolled users**	**REO**	**REC**	**PHY**	**IMA**	**REO**	**REC**	**PHY**	**IMA**
Proposed (optimal within-task threshold)	55	54	5.44%	7.74%	6.35%	7.38%	96.69%	94.89%	95.99%	95.47%
Proposed (optimal within-task threshold)	80	29	5.34%	8.41%	8.05%	7.05%	95.66%	94.54%	96.96%	97.48%
Proposed (stringent threshold)	55	54	5.57%	5.83%	4.46%	5.47%	95.91%	93.47%	95.88%	95.42%
Proposed (stringent threshold)	80	29	2.21%	2.45%	4.02%	3.69%	95.84%	93.99%	96.02%	96.19%
[2]	80	29	3.20%	4.49%	0.20%	0.56%	-	-	-	-

Notes: We tested our method with two different thresholds, an optimal one, calculated by optimising the system accuracy on the train task, and a stringent one, fixed at 87.50% patch agreement (14 patches out of 16).

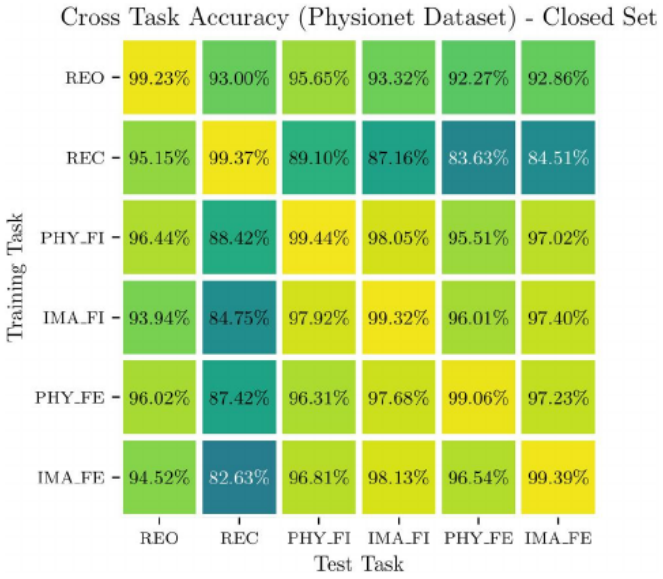

FIGURE 5 Physionet results in the closed set protocol. The train tasks are shown in the rows and the test tasks in the columns

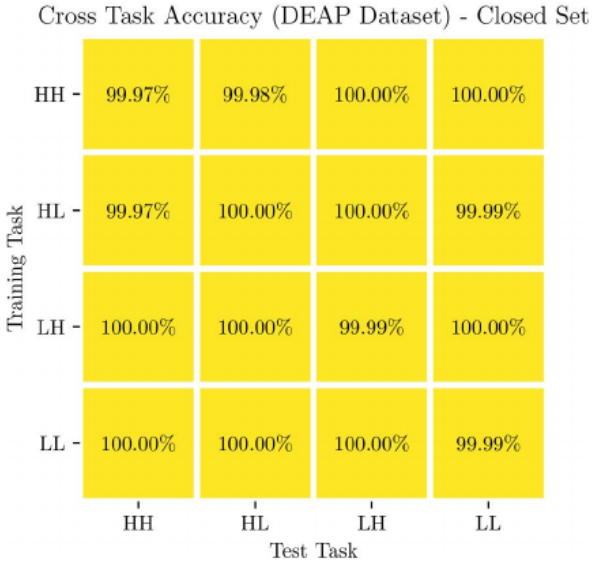

FIGURE 6 DEAP results in the closed set protocol. The train tasks are shown in the rows and the test tasks in the columns

case, for the open-set scenario. In the closed-set one, the accuracies reached a maximum of 99.26% and a minimum of 84.54%. These differences are in line with that of the SOTA works, for example, the ones reported in [10] (best cross task accuracy of 92.72%).

Whilst results in [10] are much worse than ours, Ref. [2] reported comparable values. REO and REC conditions were employed together for the system's training. Tasks PHY_* were grouped into a unique task and the same was done for the IMA_* tasks and used as the test. Accordingly, the accuracy reported was 85.40% on the PHY_* task and 87.03% on the IMA_* task. To carry out the comparison, we averaged our values by obtaining 90.16% for the PHY_* task and 89.46% on IMA_* tasks. Therefore, our approach was not only competitive with [2] but also exhibited better performance in the cross-task test.

Although resting states are considered the baseline, the REC task is the worst one (Figure 5), whether used in the training phase or in the test phase, probably due to the absence of the visual stimulus. Such configuration was not able to handle intraclass variations denoted by the other tasks. Perhaps, keeping the eyes closed during the signal acquisition reduced the interclass variations necessary to distinguish two different users. Even the REO settings are less useful in a cross-task application than in IMA and PHY tasks, as shown in [2, 10, 50]. This evidence is supported by the high performance on the DEAP dataset (Figure 6), where strong visual-stimuli-inducing emotions characterise the subject's signal.

These results support the assumption on high frequencies' informative contribution, which embed the onset of emotions and visual activity. If trained on REC tasks, during which the individual experiences fewer stimuli, the system fails to generalise and is not robust against variations. When trained in the presence of muscle activity, such as PHY_FI and PHY_FE tasks of the Physionet dataset, or visual activity, such as the DEAP dataset, the system is more robust against variation and exhibits better cross-task accuracy.

It should be worth noting that a realistic, in-the-wild use of EEG as biometric trait suggests the adoption of recordings different from that under resting state. It is true that the resting state is the configuration trying to extract the 'pure' brain signal, but this can be good for biomedical applications instead of biometric ones. This also motivates the experiment in Section 3.5.3, where we reduced the number of electrodes as usual in 'cheap' portable devices for EEG acquisition.

Figures 7 and 8 show the cross-task open-set results for the Physionet dataset with the configuration of 55–54 and 80–29 enrolled-unenrolled users, respectively. It is evident from the results that in the open set, the cross-task accuracies exhibited a drastic decrease. As previously highlighted, the REC task is the least capable of distinguishing users. In general, cross-task accuracies are particularly influenced by FNIR, therefore by genuine users who are rejected. This is particularly evident in the system trained on 80 users, with only 29 unenrolled users.

Figure 9 shows the open-set results for the DEAP dataset. The small number of users and the most stimulating tasks make the system perfectly capable of handling intraclass variations and interclass similarities. Unlike the Physionet, there are no particular differences in performance between within-task and cross-task experiments. Therefore, the audio-visual stimuli and the related associated emotions allow the system to maintain high robustness against intraclass variations. The greatest difficulties in recognition are found in the experiments involving the HL and LH tasks, characterised by high FPIR values, with peaks of 14%. This means that the chosen threshold allows a high insertion of impostors into the system. Therefore, a more stringent acceptance threshold must be set so that more patches are required to be classified. On the other hand, lowering the number of incorrectly authorised impostors

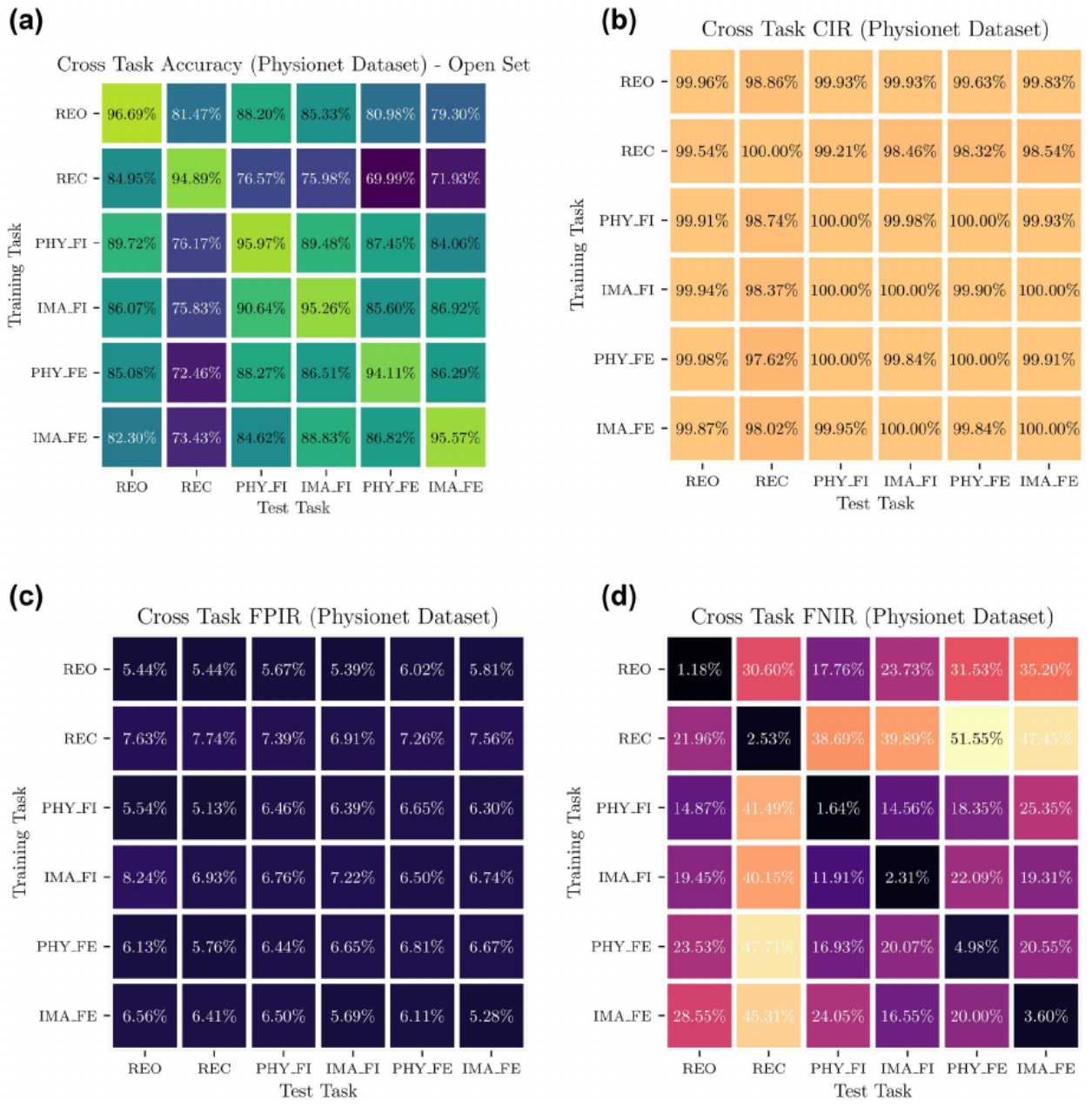

FIGURE 7 Physionet results in the open set protocol (trained on 55 users and test on 54 users)

causes an increase in the FNIR, that is, the percentage of rejected genuine users.

3.5.3 | Number of electrodes' reduction

In this section, we evaluate the effect of reducing the number of electrodes on a personal recognition system's performance.

To make a comparison with the SOTA, we replicated the same reduction applied by [2]. In particular, we analysed three electrode settings, the Cognionics QUICK-30 with 29 electrodes, the QUICK-20 with 19 electrodes and the Emotiv EPOC+ with 14 electrodes, shown in Figure 10.

The accuracies and errors in closed sets have been reported in Figure 11. Consistent with Wang et al.'s [2] findings, the reduction of electrodes and associated information results in a slight decrease in accuracy in within-task applications and a more consistent performance reduction in cross-task ones.

However, the performance reduction in the case of Wang's method [2] is more than that of the proposed method. For a system trained on REO and REC tasks and tested on IMA_* and on PHY*, Wang's is below 80% when using the 29 electrode configuration, below 60% for the 19 electrode configuration and below 50% for the 14 electrode configuration. The reduction of electrodes also worsens the performance of the system in our approach, especially in the 14-channel configuration.

The deterioration becomes unsustainable in open-set applications (Figure 12) where only the within-task results

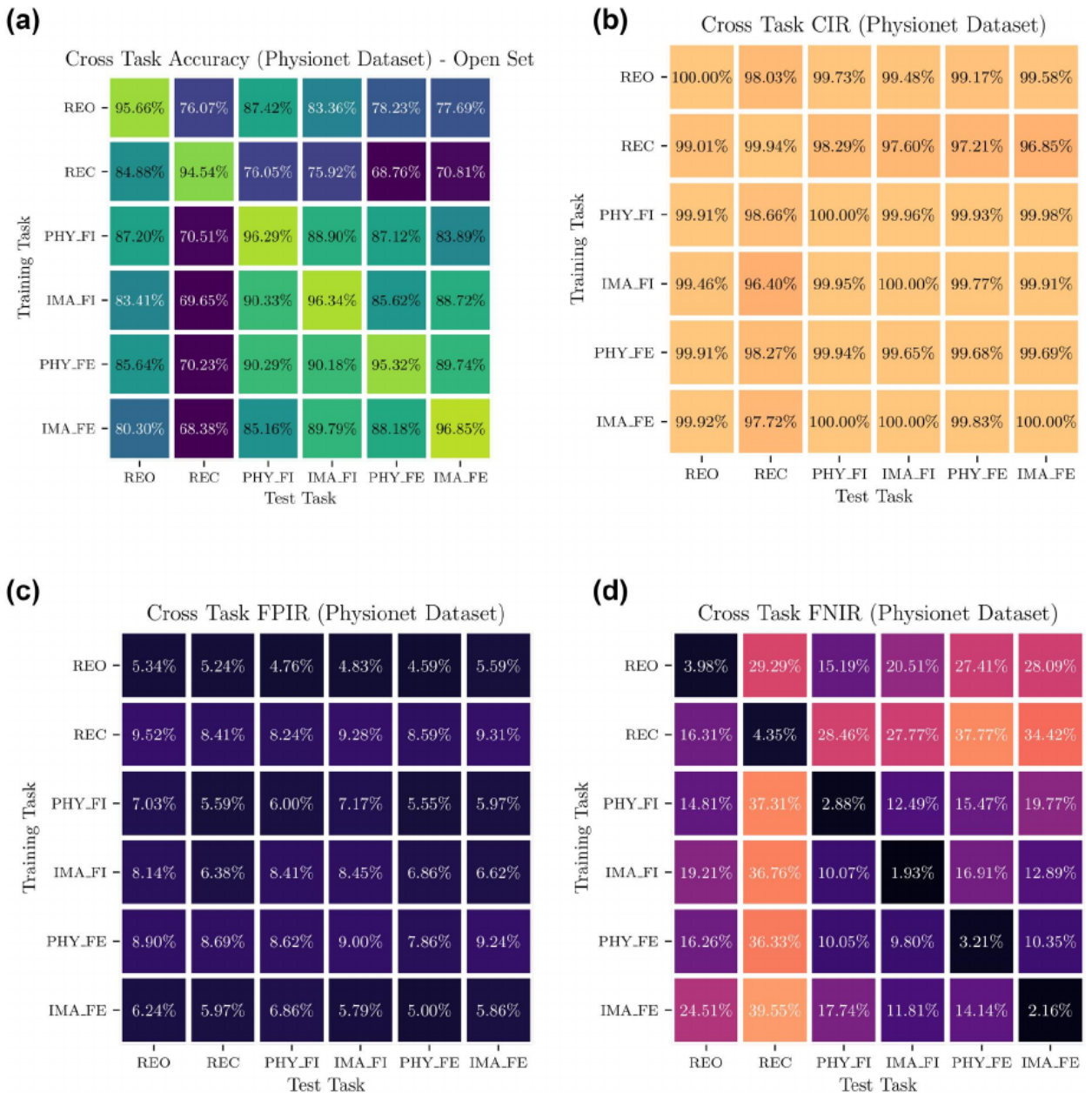

FIGURE 8 Physionet results in the open-set protocol (trained on 80 users and test on 29 users)

maintain the performance above 85% for the 29-electrode configuration and about 80% for the others.

It is important to underline that reducing the number of electrodes leads to reducing the images put in to the neural network and reducing the information embedded. We plan to explore how the information loss due to electrodes' reduction can be compensated, in future works. Among the hypotheses to be tested, there are those adopting more extended patches or reducing the population of users. If these hypotheses are not confirmed, the possible conclusion could be as follows: the task activity requires wider brain regions to be stimulated, and this discriminant information can be captured only by using more electrodes in different locations. In this case, the particular condition, if any, must be searched for, which can put an EEG signal captured with a reduced set of electrodes in a position to be useful for person recognition in a user population of a size similar to those investigated here.

3.5.4 | Processing pipelining

The system configuration for determining the processing times of a patch using our CNN model was an Intel Core i5-8300H CPU, 32 GB DDR4 of RAM and a Nvidia GeForce GTX 1050 Ti GPU.

The average processing time of a patch, calculated on a subset of 10 users of the Physionet dataset, was 59.73 ms with

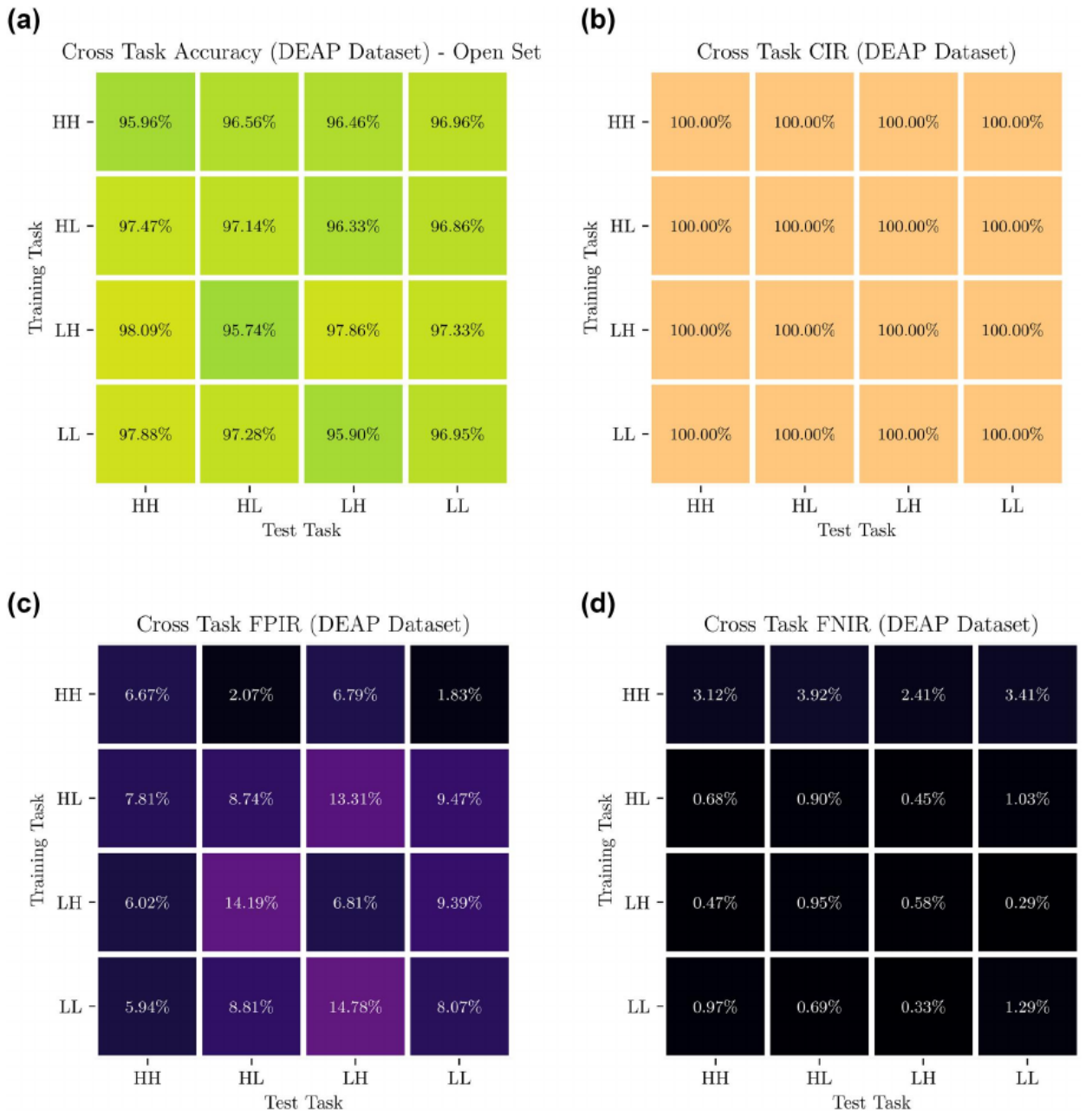

FIGURE 9 DEAP results in the open-set protocol

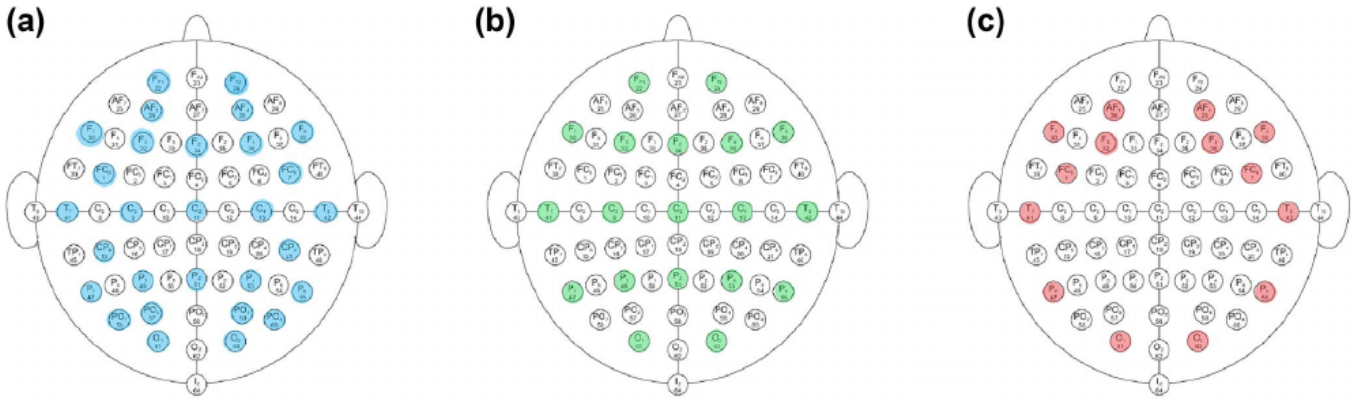

FIGURE 10 Starting with the 64-electrode Physionet configuration [44], we used three additional electrode settings: Cognionics QUICK-30 (29 electrodes) (a), QUICK-20 (19 electrodes) (b), and Emotiv EPOC+ (14 electrodes) (c) as in [2]

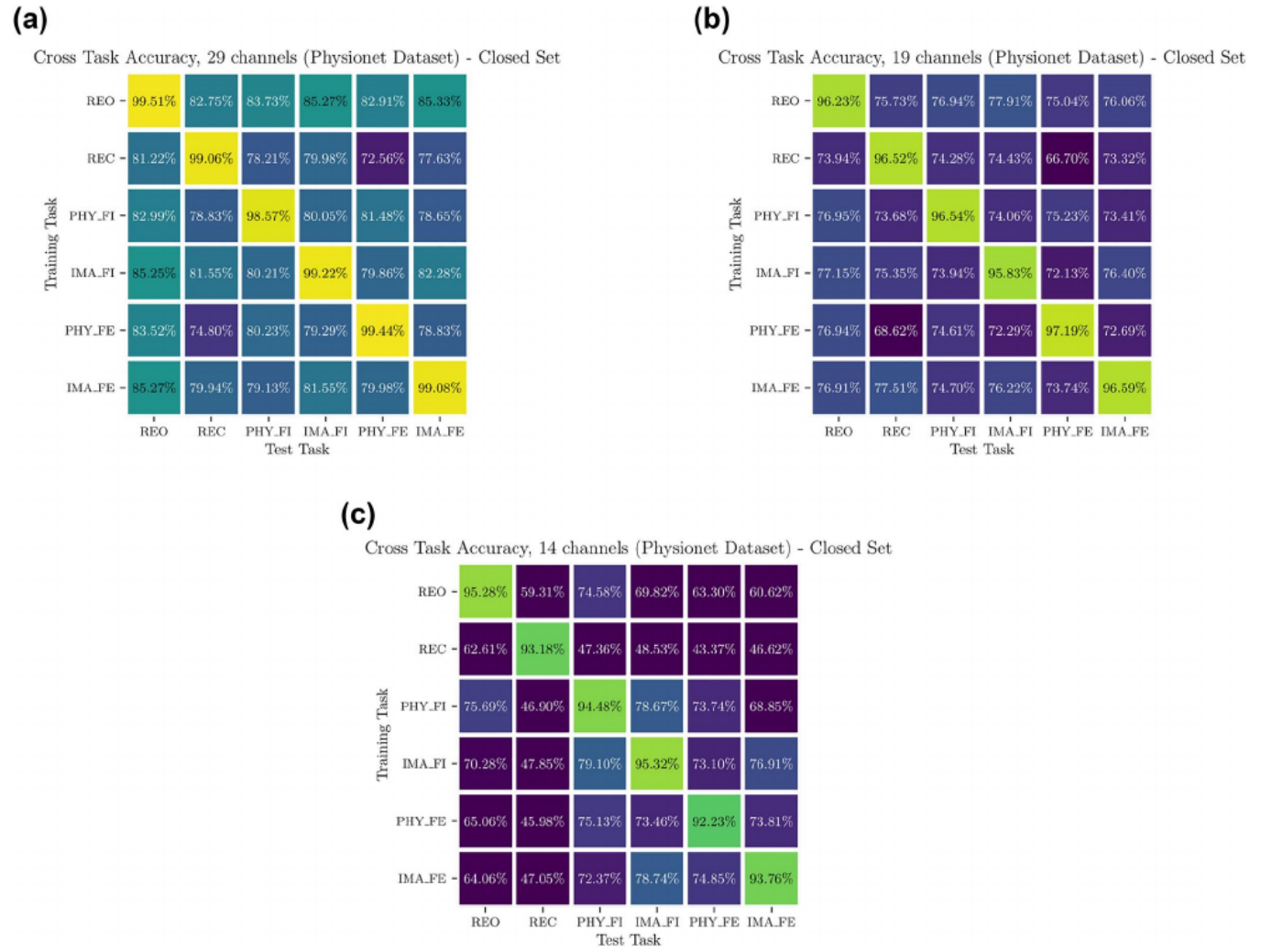

FIGURE 11 Physionet results in the closed-set protocol when the number of electrodes are reduced to 29 (a), 19 (b) and 14 (c)

a standard deviation of 3.40 ms. In particular, these are made up of 34.77 ms for filtering, 8.37 ms for normalisation and 16.45 ms for classification. Given that the processing time was slightly less than the length of the patch, we could record the next patch during the classification of the first one. This led to the pipelining of the recording and classification steps. Usually, systems that classify the epoch without the division into patches need the entire epoch time and the processing time to perform the classification.

In our case, on the other hand, the total time was equal to $(N + 1) * L$, where N is the number of patches and L is their time size. In the case of 0.063 s long patches, the total identification time was 1.063 s, which was equal to the epoch recording time plus the processing of one patch. In other words, the user could never perceive the difference between signal acquisition and the system's decision because this would take only 0.063 s more in the worst case. Since the acceptance threshold for the 'qualified majority' could be reached before all patches were processed, the total identification time was further reduced. Therefore, our approach is much faster than other SOTA methods that do not adopt the patch and qualified majority concepts.

4 | CONCLUSIONS

A personal identification system based on the decision-level fusion of very short EEG signal fragments, called patches, has been proposed. The use of patches and high frequencies of the gamma band better characterise the brain activity in the realistic waking state, obtaining high performances while keeping the identification times very low. Besides, multiple patches allow us to collect enough evidence about the individual to be recognised and, thanks to the concept of qualified majority and a threshold on the number of agreed votes, to reject uncertain subjects.

We tested the system in the worst scenarios, for enrolled and unenrolled users, cross-tasks between train and test and by reducing the number of electrodes. For the evaluation, we used two datasets to simulate different application conditions: the first one with standard resting state conditions and physical or imagined tasks and the second one with strong variations in terms of the human emotional state.

Our method outperformed other ones across realistic and challenging conditions of use. However, the system performs best with the majority of electrodes at disposal (64 for the first dataset, 32 for the second one). Further experimental

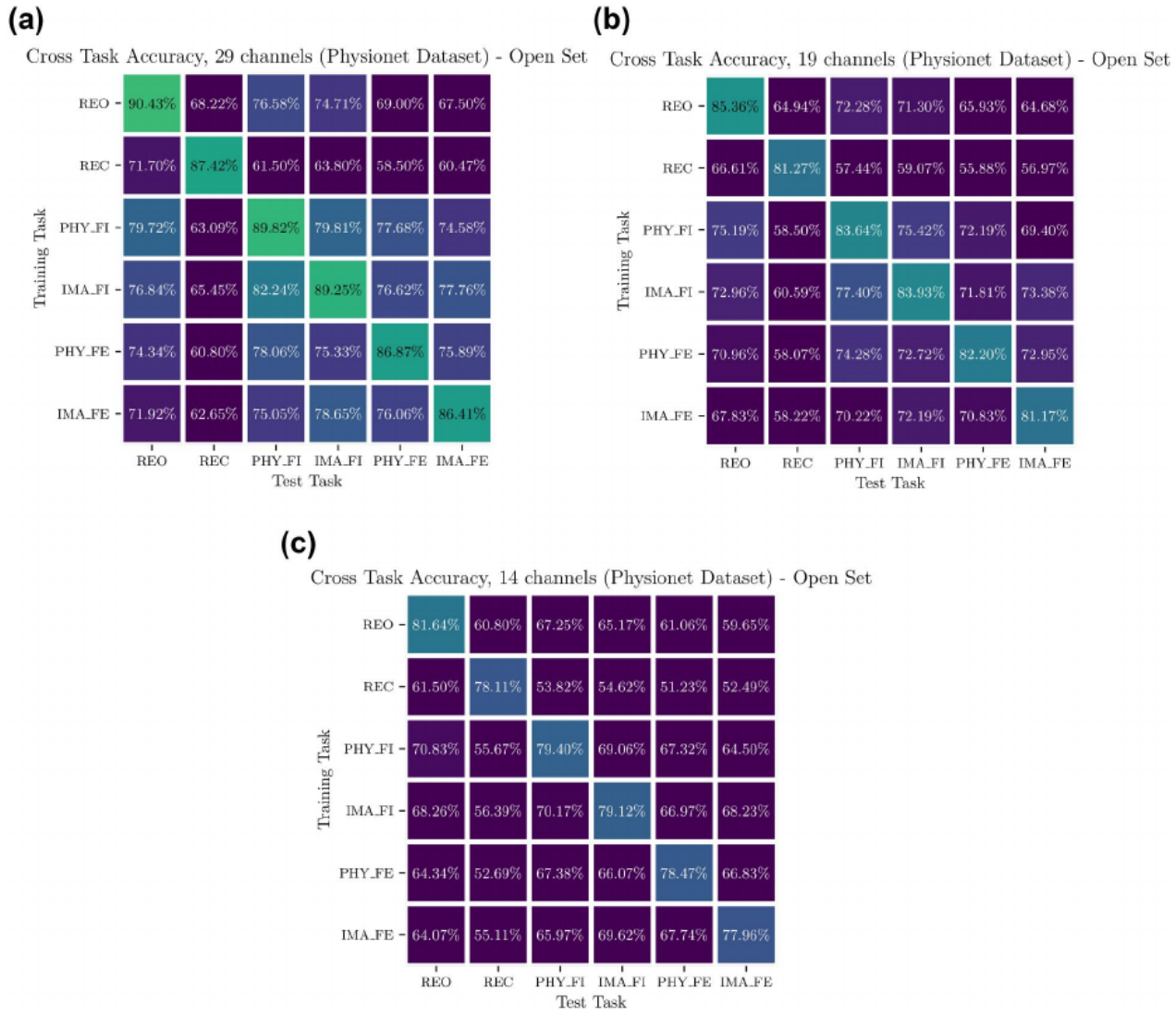

FIGURE 12 Physionet results in the open set-protocol when the number of electrodes are reduced to 29 (a), 19 (b) and 14 (c)

investigations are needed to estimate if a longer patch compensates for the information reducing due to fewer electrodes. The possibility of exploiting the multiple patches' fusion for pipelining and improving the decision process in time and accuracy added further contribution to the state of the art.

To sum up, this study contributed to two specific aspects still open in EEG personal recognition: (1) the length of the epoch and (2) the role of EEG sub-bands. In both cases, we confirmed that the epoch's length can be reduced to less than 1 s and the lowest frequency sub-bands can be kept, but their impact on the performance is not significant. This is in agreement with in-the-wild applications where the neural activity characterised by those sub-bands is not fully involved.

ORCID

Giulia Orrù https://orcid.org/0000-0002-7802-2483

REFERENCES

1. Campisi, P., La Rocca, D., Scarano, G.: EEG for automatic person recognition. Computer. 45(7), 87–89 (2012)
2. Wang, M., et al.: Convolutional neural networks using dynamic functional connectivity for EEG-based person identification in diverse human states. IEEE Trans. Inf. Forens. Secur. 14(12), 3259–3272 (2019)
3. Chan, H.L., et al.: Challenges and future perspectives on electroencephalogram-based biometrics in person recognition. Front. Neuroinf. 12, 66 (2018)
4. Maiorana, E., Campisi, P.: Longitudinal evaluation of EEG-based biometric recognition. IEEE Trans. Inf. Forens. Secur. 13(5), 1123–1138 (2018)
5. Jalaly Bidgoly, A., Jalaly Bidgoly, H., Arezoumand, Z.: A survey on methods and challenges in EEG based authentication. Comput. Secur. 93 (2020)
6. Yang, S., Deravi, F.: On the usability of electroencephalographic signals for biometric recognition: a survey. IEEE Trans. Hum. Mach. Syst. 47(6), 958–969 (2017)
7. Ma, L., et al.: Resting state EEG-based biometrics for individual identification using convolutional neural networks. In: Conference proceedings: Annual International Conference of the IEEE Engineering in Medicine and Biology Society, pp. 2848–2851. IEEE, Milan (2015)
8. Campisi, P., Rocca, D.L.: Brain waves for automatic biometric-based user recognition. IEEE Trans. Inf. Forensics Secur. 9(5), 782–800 (2014)
9. Fraschini, M., et al.: An EEG-based biometric system using eigenvector centrality in resting state brain networks. IEEE Signal Process Lett. 22(6), 666–670 (2015)

10. Fraschini, M., et al.: Robustness of functional connectivity metrics for EEG-based personal identification over task-induced intra-class and inter-class variations. Pattern Recogn. Lett. 125, 49–54 (2019). ISSN 0167-8655
11. Orrù, G., et al.: Personal identity verification by EEG-based network representation on a portable device. In: Vento, M., Percannella, G. (eds.) Computer Analysis of Images and Patterns, CAIP 2019. Lecture Notes in Computer Science, vol. 11679, pp. 164–171. Springer, Cham (2019)
12. Garau, M., et al.: Experimental results on multi-modal fusion of EEG-based personal verification algorithms. In: 2016 International Conference on Biometrics (ICB), Halmstad, pp. 1–6. (2016)
13. Bhattacharyya, A., et al.: A novel multivariate-multiscale approach for computing EEG spectral and temporal complexity for human emotion recognition. IEEE Sensor J. 21(3), 3579–3591 (2021). https://doi.org/10.1109/JSEN.2020.3027181
14. Sharma, R., Pachori, R.B., Sircar, P.: Automated emotion recognition based on higher order statistics and deep learning algorithm. Biomed. Signal Process Contr. 58 (2020). https://doi.org/10.1016/j.bspc.2020.101867
15. Gupta, V., Chopda, M.D., Pachori, R.B.: Cross-subject emotion recognition using flexible analytic wavelet transform from EEG signals. IEEE Sensor J. 19(6), 2266–2274 (2019). https://doi.org/10.1109/JSEN.2018.2883497
16. Henry, J.C.: Electroencephalography: basic principles, clinical applications, and related fields. Neurology, 67(11), 2092 (2006)
17. Satheesh Kumar, J., Bhuvaneswari, P.: Analysis of electroencephalography (EEG) signals and its categorization – a study. Procedia Eng. 38, 2525–2536 (2012). https://doi.org/10.1016/j.proeng.2012.06.298
18. Levy, W.J.: Effect of epoch length on power spectrum analysis of the EEG. Anesthesiology. 66(4), 489–495 (1987)
19. Wilaiprasitporn, T., et al.: Affective EEG-based person identification using the deep learning approach. IEEE Trans. Cogn. Dev. Syst. 12(3), 486–496. https://doi.org/10.1109/TCDS.2019.2924648
20. Das, B.B., et al.: A spatio-temporal model for EEG-based person identification. Multimed. Tool Appl. 78, 28157–28177 (2019)
21. Topçu, B., Erdogan, H.: Decision fusion for patch-based face recognition. In: 2010 20th International Conference on Pattern Recognition, Istanbul, pp. 1348–1351. (2010). https://doi.org/10.1109/ICPR.2010.333
22. Chugh, T., Cao, K., Jain, A.K.: Fingerprint spoof buster: use of minutiae-centered patches. IEEE Trans. Inf. Forensics Secur. 13(9), 2190–2202 (2018). https://doi.org/10.1109/TIFS.2018.2812193
23. He, L., et al.: Multi-patch convolution neural network for iris liveness detection. In: 2016 IEEE 8th International Conference on Biometrics Theory, Applications and Systems (BTAS), Niagara Falls, NY, pp. 1–7. (2016). https://doi.org/10.1109/BTAS.2016.7791186
24. Estrada, E., et al.: EEG feature extraction for classification of sleep stages. In: The 26th Annual International Conference of the IEEE Engineering in Medicine and Biology Society, San Francisco, pp. 196–199. (2004). https://doi.org/10.1109/IEMBS.2004.1403125
25. Åkerstedt, T., Gillberg, M.: Subjective and objective sleepiness in the active individual. Int. J. Neurosci. 52(1–2), 29–37 (1990). https://doi.org/10.3109/00207459008994241
26. Muthukumaraswamy, S.: High-frequency brain activity and muscle artifacts in MEG/EEG: A review and recommendations. Front. Hum. Neurosci. 7, 138 (2013). https://doi.org/10.3389/fnhum.2013.00138
27. Amo, C., et al.: Analysis of gamma-band Activity from human EEG using empirical mode decomposition. Sensors. 17, 989 (2017)
28. Yang, K., et al.: High gamma band EEG closely related to emotion: evidence from functional network. Front. Hum. Neurosci. 14, 89 (2020). https://doi.org/10.3389/fnhum.2020.00089
29. Poulos, M., Rangoussi, M., Alexandris, N.: Neural network based person identification using EEG features. In: 1999 IEEE International Conference on Acoustics, Speech, and Signal Processing. Proceedings. ICASSP99 (Cat. No.99CH36258), Phoenix, vol. 2, pp. 1117–1120. (1999)
30. Safont, G., et al.: Combination of multiple detectors for EEG based biometric identification/authentication. In: 2012 IEEE International Carnahan Conference on Security Technology (ICCST), Boston, pp. 230–236. (2012)
31. Poulos, M., et al.: Parametric person identification from the EEG using computational geometry. In: ICECS'99. Proceedings of ICECS '99. 6th IEEE International Conference on Electronics, Circuits and Systems (Cat. No.99EX357), Pafos, Cyprus, vol. 2, pp. 1005–1008. (1999)
32. Dan, Z., Xifeng, Z., Qiangang, G.: An identification system based on portable EEG acquisition equipment. In: 2013 Third International Conference on Intelligent System Design and Engineering Applications, Hong Kong, pp. 281–284. (2013)
33. Yang, S., Deravi, F.: Wavelet-based EEG preprocessing for biometric applications. In: 2013 Fourth International Conference on Emerging Security Technologies, Cambridge, pp. 43–46. (2013)
34. Yang, S., Deravi, F.: Novel HHT-based features for biometric identification using EEG signals. In: 2014 22nd International Conference on Pattern Recognition, Stockholm, pp. 1922–1927. (2014). https://doi.org/10.1109/ICPR.2014.336
35. La Rocca, D., et al.: Human brain distinctiveness based on EEG spectral coherence connectivity. IEEE Trans. Biomed. Eng. 61(9), 2406–2412 (2014)
36. Mao, Z., Yao, W.X., Huang, Y.: EEG-based biometric identification with deep learning. In: 2017 8th International IEEE/EMBS Conference on Neural Engineering (NER), Shanghai, pp. 609–612. (2017)
37. Das, R., Maiorana, E., Campisi, P.: Visually evoked potential for EEG biometrics using convolutional neural network. In: 2017 25th European Signal Processing Conference (EUSIPCO), Kos, pp. 951–955. (2017)
38. El-Fiqi, H., et al.: Convolution neural networks for person identification and verification using steady state visual evoked potential. In: 2018 IEEE International Conference on Systems, Man, and Cybernetics (SMC), Miyazaki, Japan, pp. 1062–1069. (2018)
39. Sun, Y., Lo, F.P.-W., Lo, B.: EEG-based user identification system using 1D-convolutional long short-term memory neural networks. Expert Syst. Appl. 125, 259–267 (2019)
40. Geng, C., Huang, S., Chen, S.: Recent advances in open set recognition: a survey. IEEE Trans. Pattern Anal. Mach. Intell. (2020)
41. Bendale, A., Boult, T.E.: Towards open set deep networks. In: 2016 IEEE Conference on Computer Vision and Pattern Recognition (CVPR), pp. 1563–1572. (2016). https://doi.org/10.1109/CVPR.2016.173
42. Singh, M., Singh, R., Ross, A.: A comprehensive overview of biometric fusion. Inf. Fusion. 52, 187–205 (2019)
43. Kittler, J., et al.: On combining classifiers. IEEE Trans. Pattern Anal. Mach. Intell. 20(3), 226–239 (1998). https://doi.org/10.1109/34.667881
44. Goldberger, A.L., et al.: PhysioBank, PhysioToolkit, and PhysioNet: components of a new research resource for complex physiologic signals. Circulation. 101(23), E215–E220 (2000)
45. Schalk, G., et al.: BCI2000: A general-purpose brain-computer interface (BCI) system. IEEE Trans. Biomed. Eng. 51(6), 1034–1043 (2004)
46. Koelstra, S., et al.: DEAP: A database for emotion analysis using physiological signals. IEEE Trans. Affect. Comput. 3(1), 18–31 (2012). https://doi.org/10.1109/T-AFFC.2011.15
47. Barrett, L.F., Russell, J.A.: The structure of current affect: controversies and emerging consensus. Curr. Dir. Psychol. Sci. 8(1), 10–14 (1999). https://doi.org/10.1111/1467-8721.00003
48. International Organization for Standardization: ISO/IEC 19795-1: Information Technology—Biometric Performance Testing and Reporting—Part 1: Principles and Framework (2006)
49. Li, S.Z., Jain, A.: Encyclopedia of Biometrics. Springer Publishing Company Incorporated (2015)
50. Yang, S., Deravi, F., Hoque, S.: Task sensitivity in EEG biometric recognition. Pattern Anal. Appl. 21, 105–117 (2016)

How to cite this article: Panzino, A., et al.: EEG personal recognition based on 'qualified majority' over sign al patches. IET Biometrics. 1–16 (2021). https://doi.org/10.1049/bme2.12050